Journal of
Nanoscience and Nanotechnology
Vol. 8, 1–7, 2008

Controlling the Catalyst During Carbon Nanotube Growth

J. Robertson[1,*], S. Hofmann[1], M. Cantoro[1], A. Parvez[1], C. Ducati[1], G. Zhong[1], R. Sharma[2], and C. Mattevi[3]

[1] *Department of Engineering, University of Cambridge, Cambridge CB3 0FA, UK*
[2] *Center for Solid State Science, Arizona State University, Tempe AZ85287-1704, USA*
[3] *Lab Nazionale TASC-INFM, I-34012 Trieste, Italy*

We have recently been able to grow single-walled carbon nanotubes by purely thermal chemical vapour deposition (CVD) at temperatures as low as 400 C. This has been achieved by separating the catalyst pre-treatment step from the growth step. In the pre-treatment step, a thin film catalyst is re-arranged into a series of nano-droplets, which are then the active catalysts. Both steps have been studied by *in-situ* environmental transmission electron microscopy and X-ray photoemission spectroscopy. We have also studied the catalyst yield, the weight of nanotubes grown per weight of transition metal catalyst. Using very thin layers of Fe on Al_2O_3 support in a remote plasma-assisted CVD, we have achieved yields of order 100,000. This may be due to control of catalyst poisoning by ensuring an etching path.

Keywords: Carbon Nanotubes, Growth, Catalysts.

RESEARCH ARTICLE

1. INTRODUCTION

Chemical vapour deposition (CVD) has emerged as the preferred method to produce carbon nanotubes, not only in bulk, but also for electronic applications where they must be produced in specific patterns on a substrate. This process has been optimised in various ways, for yield, purity or chiral selectivity. Here, we consider what limits growth at lower temperatures and also the yield. There are also questions about how the nucleation and growth occurs at a microscopic level, such as what is the chemical and physical nature of the catalyst–metal or oxide or carbide, and solid or liquid.

2. LOW TEMPERATURE GROWTH

The growth of carbon nanotubes is a thermally activated process; it becomes faster at high temperatures. But which elementary step actually limits the growth? This could be the dissociation of the gas precursor on the catalyst surface, the diffusion of carbon through or over the catalyst, the precipitation of carbon to form the nanotube, or the activation of the catalyst into its active state, as in Figures 1(a, b).

The first study of growth mechanisms of carbon nanofibres or filaments by Baker et al.[1] noted that the activation energy of growth using Fe, Co, Ni or Cr as catalyst was similar to the activation of carbon diffusivity through the bulk metal. The diffusivity is the product of the carbon solubility and the carbon diffusion coefficient, both of which are activated. These activation energies are well known from the metallurgical literature.[2–5]

Growth rate studies for multi-walled carbon nanotubes (MWNTs) have found a range of activation energies.[6–11] Lee,[6] Puretzky[8] and Zhu[9] found an activation energy of 1.5–2.2 eV for CVD growth of MWNTs with Fe catalyst over a restricted temperature range. Ducati et al.[10] derived a lower value of ∼1.2 eV for CVD with Ni catalyst, as in Figure 2.

Plasma-assisted processes are often used in microelectronics to lower processing temperatures. This is because the plasma dissociates the reaction precursor, even before it interacts with the catalyst surface. Thus, PECVD allows nanotubes to been grown at lower temperatures.[11–20] For example, Hofmann et al.[12,13] observed that the low-power plasma-enhanced chemical vapor deposition (PECVD) of MWNTs using Ni, Co or Fe as a catalyst and acetylene/ammonia mixture as growth gas gave a growth activation energy of order 0.23 eV (Fig. 2), which is much lower than that found by simple thermal CVD. This has enabled MWNT growth to be achieved at much lower temperatures than in thermal CVD. Minea et al.[14] used microwave PECVD to further lower growth temperatures, while achieving a reasonable nanotube quality.

*Author to whom correspondence should be addressed.

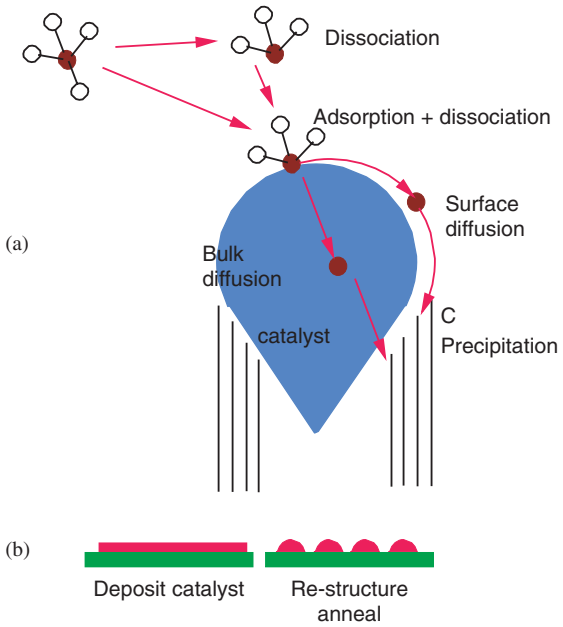

Fig. 1. Possible elementary steps in the growth of carbon nanotubes. Tip growth is illustrated. (b) In addition, catalyst re-structuring/activation.

Techniques such as hot-wire deposition are related to PECVD,[21] as they also mildly dissociate the gas species. One should be aware that plasmas can cause local heating of the substrate,[22] so that the effective growth temperatures can exceed those quoted by the authors. In our work,[12, 13] low plasma powers are used, so that temperature data are reasonably reliable, and have recently been confirmed by pyrometry. There are other reports of nominal room temperature growth where the active temperature is much higher.[20, 23]

The growth process is known to involve a metallic catalyst which is transformed into a series of nano-particles during or before the growth step. The catalyst is deposited as a thin film on the substrate, usually Si. The Si is usually coated with SiO_2 or some other diffusion barrier layer. In catalysis, this layer is called the 'support.' During heating to the growth temperature, or otherwise, the thin film restructures itself into a discontinuous film of catalyst nano-particles.[11, 13, 18] The restructuring occurs by de-wetting, aided a lack of adhesion between metal and support. Then, the nanotube grows by either tip or root growth. Growth occurs in a gas mixture; in CVD it is usually a hydrocarbon diluted by hydrogen or similar. In PECVD it is a hydrocarbon plus a gas whose role is an etchant of any parallel deposition of amorphous carbon.[18] Ammonia is an easier source of atomic hydrogen than molecular H_2 itself.

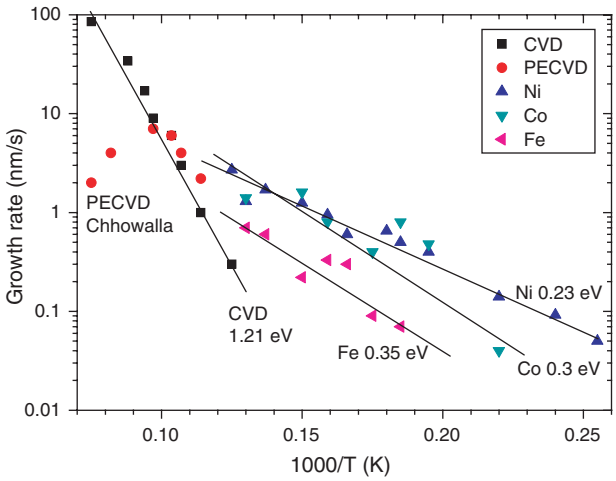

Fig. 2. Growth rates of MWNTs grown by CVD[10] and by PECVD, after Chhowalla[11] and Hofmann.[12, 13]

Thus, overall, growth of nanotubes can involve three *sequential* processes,

- re-structuring of the catalyst,
- dissociation of the growth species into carbon on the catalyst surface and
- diffusion of the carbon to the growth site to form the nanotube.

Each of these processes can be thermally activated. But which is rate-limiting? For one process to be rate-limiting, *both* other processes must be faster, and usually with a lower activation energy. Baker[1] suggests that bulk diffusion of C through the metal is rate-limiting for thermal CVD of nanofibres. The 1.5–2.2 eV activation energy found for MWNT CVD[6–9] is also consistent with bulk diffusion. In thermal CVD, it is assumed that the precursor dissociation on the catalyst surface is fast, and also that the surface diffusion path on the catalyst may be blocked by excess amorphous carbon formation. On the other hand, in PECVD it was proposed that the plasma acts to dissociate the feedstock and also keep the catalyst surface clear of amorphous C by etching.[12] Thus, the precursor dissociation is always fast in PECVD. The similarity of the PECVD growth activation energy of 0.23 eV to the known surface diffusion energy of carbon on Ni led to the suggestion that the PECVD of nanotubes was limited by surface diffusion of C on the Ni, whereas it is bulk diffusion limited in thermal CVD.[12]

Hofmann et al.[24] calculated the activation energy of both bulk and surface diffusion of C on Ni. The surface diffusion has a much lower activation energy than bulk diffusion, of order 0.3–0.35 eV, depending on face. They and Raty et al.[25] noted that surface diffusion becomes a more likely path when the catalyst particle becomes as small as it is for SWNT growth. Thus overall, diffusion can be a low activation path in the growth of SWNTs and narrow MWNTs. (Note that the catalyst particle tends to have a similar diameter to the resulting nanotube in CVD, whether SWNT or MWNT, whereas in high temperature arc or laser processes, many SWNTs tend to grow from one catalyst particle.[26])

RESEARCH ARTICLE

But what about catalyst re-structuring? The catalyst films are deposited by sputtering or evaporation. These films tend to grow in island mode, especially on oxide supports, and can be continuous or discontinuous, depending on their thickness. A restructuring step is used to convert these films into an array of nano-particles of similar, smaller size.

AFM measurements after catalyst deposition and re-structuring but before growth showed that a plasma is significant in allowing re-structuring to occur at much lower temperatures.[13] Thus, low temperature PECVD growth becomes possible because re-structuring and dissociation are low energy processes under plasma conditions.

What temperatures can re-structuring be expected to occur? Melting would allow de-wetting to occur very easily. However, processing temperatures are well below the melting point. Plastic deformation of solid ultra-thin films is possible at rather low homologous temperatures.[27–29] This led us to consider separating the re-structuring and growth steps in time for CVD, Figure 3. The thin film catalyst is first heated to a re-structuring temperature, either in a vacuum or more usually in a reducing ambient such as ammonia. AFM measurements found that the ambient gas, even at low pressures, has a strong effect on the particle size. This effect is particularly useful for Fe films, which oxidise during transfer from the sputter chamber to the growth chamber. The size change during reduction

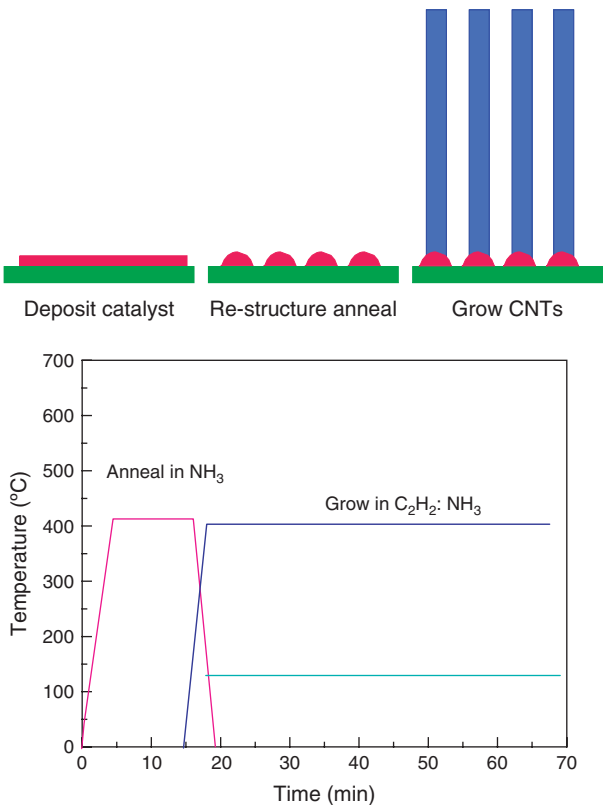

Fig. 3. Separating the re-structuring and growth steps for base growth, (a) schematically, and (b) in terms of gas flows.

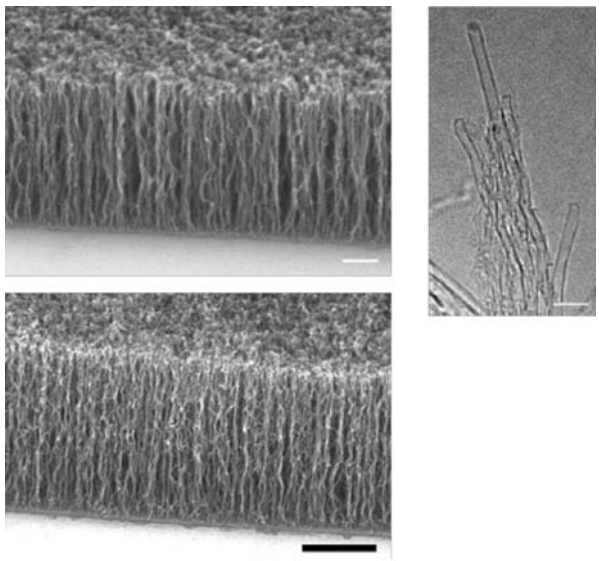

Fig. 4. SWNT mats grown by CVD, after Cantoro et al.[30]

converts a continuous film into a very particulate film. After restructuring, but still in the vacuum chamber, the growth gas mixture is then admitted, and the second growth stage occurs.

This process flow allows catalyst restructuring to occur at unexpectedly low homologous temperatures. Using this, we have been able to grow MWNTs by thermal CVD to below 300 C. Cantoro et al.[30] were able to grow SWNTs at 400 C or below, Figure 4. In these cases, both restructuring and growth was carried out below 400 C.

These arguments suggest that, provided that the growth gas is not methane, dissociation of the growth precursor is not costly, surface diffusion costs only 0.3 eV or so, so that catalyst re-structuring can be the most costly step of this process sequence. It is thus necessary to carry it out in an appropriate manner. Perhaps, without a prior re-structuring step, carburisation inhibits the catalyst re-structuring.

3. *IN-SITU* STUDIES

These observations were confirmed by direct *in-situ* studies using an environmental transmission electron microscope (ETEM) and an environmental X-ray photoemission (XPS) study. *In-situ* studies are value in understanding growth mechanisms.[31–38] However, some images were taken from videos and have a lower resolution than *ex-situ* images, which cannot easily be improved at present.

During the NH_3 ambient step, the ETEM images and videos clearly show the catalyst of 1 nm Ni on SiO_2 re-structuring from a thin film into a series of balls, Figure 5, while remaining crystalline with clear lattice planes.[35] This confirms that pronounced catalyst restructuring is possible at low homologous temperatures for a solid catalyst. Similar effects were also seen by Hansen.[31]

Figure 6 shows the growth of MWNTs in C_2H_2 and NH_3 ambient, by tip growth.[35] During growth, the MWNT

RESEARCH ARTICLE

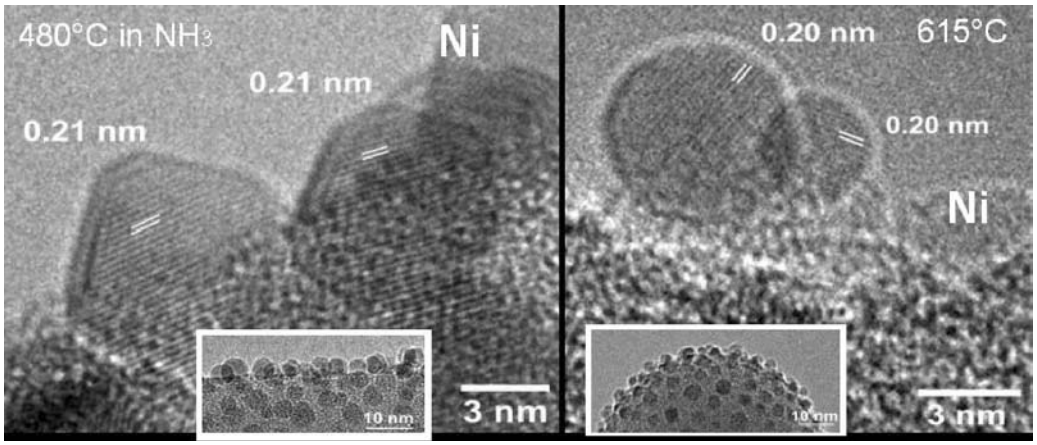

Fig. 5. ETEM images of Ni nanoparticles on SiO_x covered silica, restructured at 480 C and 615 C in vacuum (10^{-6} mbar).

takes a number of sharp turns. The surrounding graphitic walls appear to deform the catalyst nano-particle that is embedded in its tip. Helveg et al.[32] found a similar effect. But the catalyst remains crystalline during this process. Its small size means that rapid plastic deformation is possible.

Acetylene is the most effective growth precursor for nanotube growth in molecular beam experiments.[39] Acetylene has a strongly exothermic decomposition to carbon. Thus, it has been suggested that a temperature gradient could drive C diffusion,[1] but this was later discounted.[40] It was also suggested that heat release could melt the catalyst particle. However, the ETEM images show that the catalyst remains solid, Figure 7.

Figure 8 shows a short SWNT having nucleated from a catalyst droplet. The graphitic planes tend to lie parallel to the edges of the catalyst particle, as also seen by Zhu.[38]

Some workers argue that SWNTs can only grow if the catalyst is liquid or liquid-like at its surface.[41] This is probably true for the arc or laser processes, but we believe not necessary for CVD. There is a large depression of melting point in small particles by the Gibbs-Thomson effect,[42, 43] and a lowering also occurs due to eutectics. The ETEM images show that the catalyst particles remain solid during our conditions, so that a molten catalyst is not a prerequisite. Video images of the various growth processes are shown in Ref. [35].

There is debate about the chemical nature of the catalyst, whether it is the metal, the oxide or the carbide. Fe carbides are metastable and Ni carbides are unstable. TEM analysis after growth can find a Fe carbide residue,[12] which might have formed by rapid quenching. Many workers have used Fe nitrates or similar as precursors for Fe catalyst. These dissociate to Fe oxide and then we believe to Fe metal. However, an Fe oxide catalyst is a possibility.

In-situ XPS of the Fe and C core levels shows the chemical state of the catalyst at the start and during growth.[33] The data suggest that Fe is in metallic form, although further work is needed. As growth starts, the C 1s level

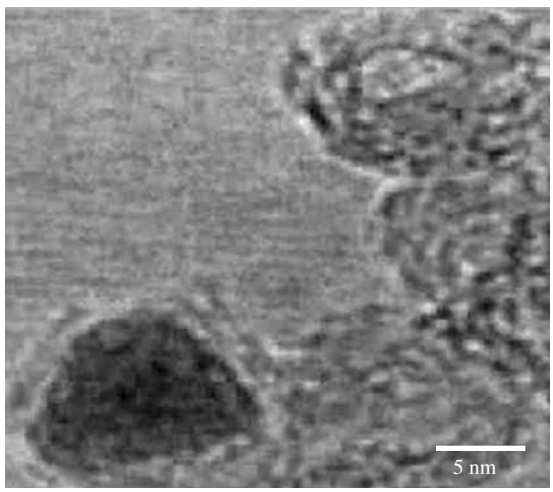

Fig. 6. Growth sequence of a MWNT growing by tip growth. 2 nm of Ni catalyst on SiO_x growing in 3:1 NH_3/C_2H_2 at 1.3 mbar total pressure at 480 °C.

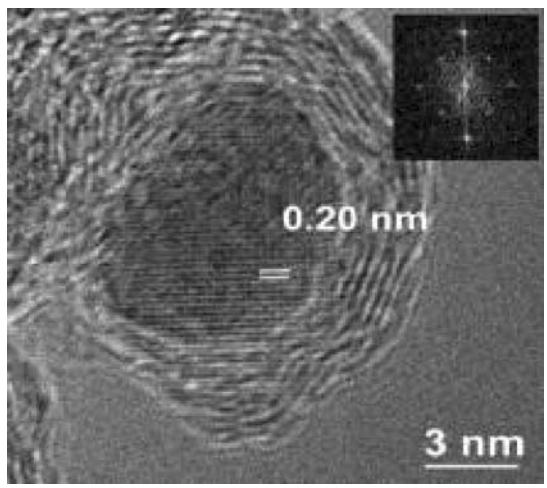

Fig. 7. Catalyst particle remains crystalline after growth has terminated, but in acetylene ambient. 360 C, 3:1 C_2H_2/NH_3 at 1.3 mbar total pressure.

RESEARCH ARTICLE

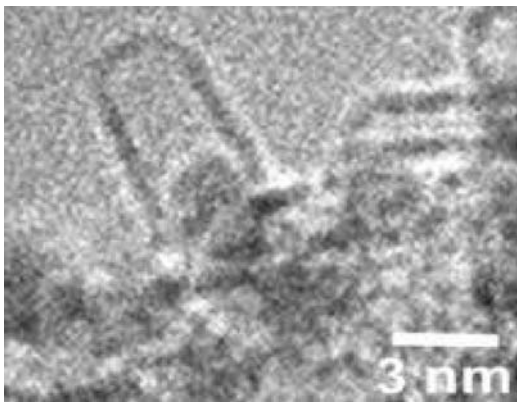

Fig. 8. Early stage of growth of a SWNT from a catalyst particle at 615 C and 8×10^{-3} mbar C_2H_2.

shows a carbide phase for 100 secs. This peak then disappears as the main graphitic peak grows, Figure 9. This suggests that the carbide phase in etched away and replaced by the graphitic phase. Note that the nanotube film is discontinuous. If a continuous over-layer was grown, then the carbide peak could be buried underneath the graphitic layer, but for a discontinuous film this is not the case. Other groups found oxide.[34]

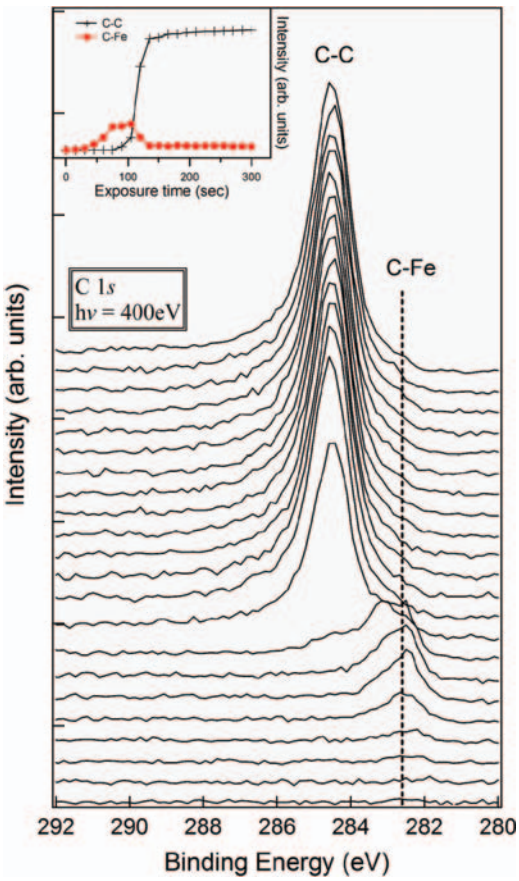

Fig. 9. Evolution of carbon 1s spectra during growing nanotubes for realistic catalyst, from Ref. [35].

4. GROWTH KINETICS AND CATALYST POISONING

A number of applications require bulk production or high purity production. The vertically aligned nanotube mats are of great interest for this, and also for studies of growth kinetics. A number of workers are able to make MWNT mats. Stop-go sequences show that these grow by base growth.[44–47] The best results occur for an Fe catalyst on Al_2O_3 support.

A number of workers have been able to grow SWNTs mats.[46–64] Maruyama et al.[44,45] first grew such SWNT by thermal CVD using methanol as growth gas, then ethanol. Murakami et al.[46] were able to grow SWNT mats by this alcohol CVD route. OH groups were believed to be useful to inhibit catalyst poisoning. Then Hata et al.[51–54] were able to grow very thick (>2 mm) SWNTs mats, by thermal CVD using diluted ethene plus a very small amount of water as growth gas. The catalyst is Fe on Al_2O_3. The water was said to act as a mild etchant of any amorphous carbon coating that might cover the catalyst nano-particle. The mat height was found to grow then saturate according to an exponential time evolution.[52] Noda et al.[55] were recently able to repeat the role of water although many have not.

Zhong et al.[56–59] have also grown thick SWNT mats using a remote microwave plasma system, Figure 10. This is called a point-arc plasma in that a point is used to localise the plasma ball away from the substrate. The catalyst is a trilayer, Al_2O_3 on Fe on Al_2O_3. The thin Al_2O_3 probably acts to further inhibit Fe sintering. The growth gas is methane. The growth is found to follow linear or quadratic kinetics, depending on the patterning of the catalyst on the substrate, Figure 11. There is linear growth kinetics if the pattern size is small. Stop-start sequences show the growth is base growth. There is no growth without a plasma, showing that methane itself is not the active species. The growth species is likely to be acetylene produced in the plasma. It is proposed that the growth can be limited by diffusion of growth species through the already grown mat to the base growth location. It is a diffusion transitional regime (related to Knudsen flow). Zhu et al.[60] has also observed diffusion-limited growth kinetics.

Geohegan et al.[61] have also produced mats. They use ferrocene to give continued growth. This is a little different to those using only a single thin film catalyst.

Thus, we have various cases of thick SWNT mat growth with different conditions. In each case, the catalyst is extremely efficient and does not easily poison. The role of water or alcohol as mild etchants is likely, although it has been debated.[62] In the remote plasma case, the plasma creates atomic hydrogen which has sufficient path length to act as etchant of amorphous C on the mat surface. The diffusion-limited growth can also act to keep the carbon activity at the catalyst surface at the base to a low value.

In Hata's case, the catalyst is Fe on Al_2O_3 and it is extremely active.[54] A claimed 86% of nanoparticles

RESEARCH ARTICLE

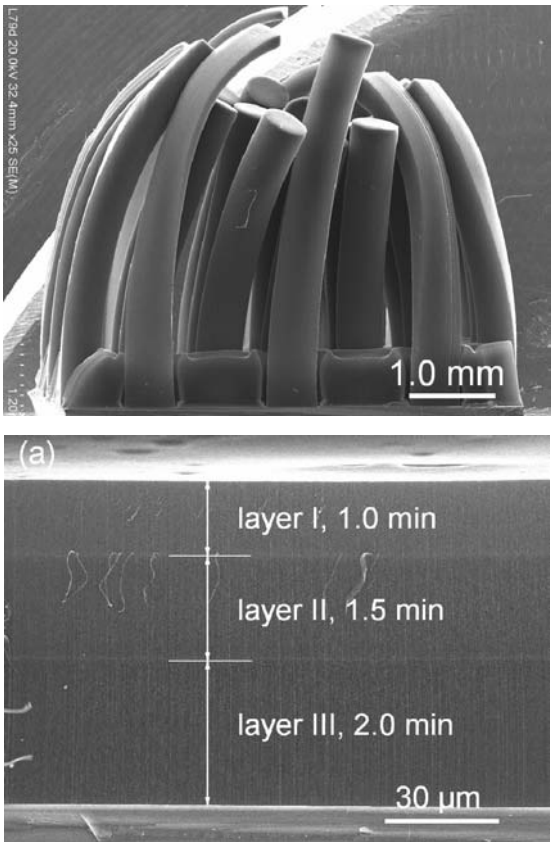

Fig. 10. Patterned arrays of thick SWNT mats, and a stop-start growth sequence.

nucleate nanotubes. The nanotube diameter is quite large, larger than typical in HiPCO material. The nanotubes show a range of diameters, from SWNTs to double walled, to narrow MWNTs.[53] But the most remarkable property is that say 0.5 nm of Fe gives rise to 2–5 mm high mats. Depending on the mat density, this is of order 10^5 catalyst efficiency defined as SWNT mass/catalyst mass. If the water truly etches amorphous and other graphitic carbon, then the material is purer than most other forms. This

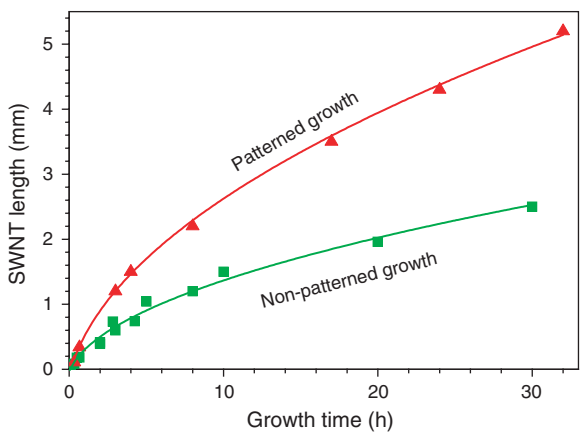

Fig. 11. Growth kinetics of SWNT mat from the remote microwave PECVD.[59]

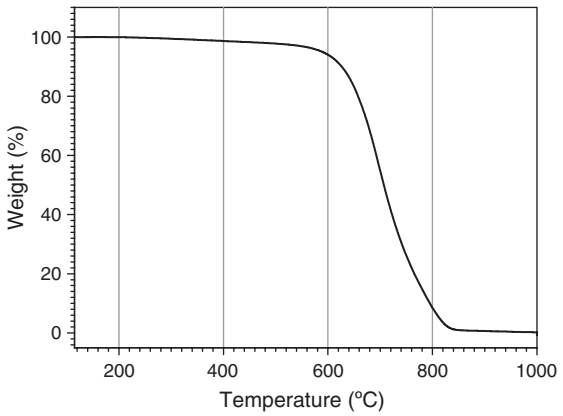

Fig. 12. Thermo-gravimetric analysis data for Zhong's mats.[58]

is a large advantage for applications where redox metals should be avoided like super-capacitors.

The catalyst is also extremely efficient in Zhong's case,[58] of order 10^5 times. The mat density is found to of order 0.06 g/cm^3 which is equivalent to a nanotube spacing of 3 nm. Thermo-gravimetric analysis (TGA) in air shows that the burn off occurs at a reasonably high and narrow temperature range, Figure 12. These results have now been reproduced at Cambridge using a conventional microwave PECVD system, where the plasma ball is again localised off the substrate. Thus the remote property is the critical aspect. As in Hata's case, we find by Raman that the tubes have a wide range of diameters from 0.8 nm to at least 1.8 nm, with most chiralities represented.

5. SUMMARY

We have summarised our work on low temperature growth of MWNTs and MWNTs. It is argued that if the processes of C diffusion and precursor diffusion can be made to have low activation energy, then catalyst re-structuring becomes the rate limiting step. Thus, lower temperature growth is achieved by having a prior step for catalyst re-structuring in an ambient without growth gas. *In-situ* ETEM and XPS measurements confirm the ideas that developed about how catalyst nano-particles behave before and during growth. In our conditions, the catalyst remains crystalline and solid, but is strongly deformable. The active catalyst is the metal.

Acknowledgments: The authors are grateful to many coworkers G. Du, C. Cepek, S. Pisana, F. Cervantes, A. C. Ferrari, R. Dunin-Borkowski, S. Lizzit, L. Petaccia, and A. Goldoni.

References and Notes

1. R. T. K. Baker, P. S. Harris, R. B. Thomas, and R. J. Waite, *J. Catal.* 30, 86 **(1973)**.
2. R. P. Smith, *Trans AIME* 224, 105 **(1962)**.
3. R. P. Smith, *Trans AIME* 236, 1224 **(1966)**.
4. R. P. Smith, *Trans AIME* 230, 476 **(1964)**.

5. S. Diamond and C. Wert, *Trans AIME* 239, 705 **(1967)**.
6. Y. T. Lee, J. Park, Y. S. Choi, H. Ryu, and H. J. Lee, *J. Phys. Chem. B* 106, 7614 **(2002)**.
7. D. B. Geohegan, A. A. Puretzky, I. N. Ivanov, S. Jesse, G. Eres, and J. Y. Howe, *App. Phys. Lett.* 83, 1851 **(2003)**.
8. A. A. Puretzky, D. B. Geohgean, S. Jesse, and I. M. Ivanov, and G. Eres, *App. Phys. A* 81, 223 **(2005)**.
9. L. Zhu, J. Xu, F. Xiao, H. Jiang, D. W. Hess, and C. P. Wong, *Carbon* 45, 344 **(2007)**.
10. C. Ducati, I. Alexandrou, M. Chhowalla, G. A. J. Amaratunga, and J. Robertson, *J. App. Phys.* 92, 3299 **(2002)**.
11. M. Chhowalla, K. B. K. Teo, C. Ducati, N. L. Rupesinghe, G. A. J. Amaratunga, A. C. Ferrari, D. Roy, J. Robertson, and W. I. Milne, *J. Appl. Phys.* 90, 5308 **(2001)**.
12. S. Hofmann, C. Ducati, B. Kleinsorge, and J. Robertson, *Appl. Phys. Lett.* 83, 135 **(2003)**.
13. S. Hofmann, M. Cantoro, B. Kleinsorge, C. Casiraghi, A. Parvez, J. Robertson, and C. Ducati, *J. Appl. Phys.* 98 **(2005)**.
14. T. M. Minea, S. Point, A. Granier, and M. Touzeau, *App. Phys. Lett.* 855, 1244 **(2004)**.
15. Y. M. Li, A. Javey, and H. J. Dai, *Nano Lett.* 4, 317 **(2004)**.
16. Y. S. Min, E. J. Bae, B. S. Oh, D. Kang, and W. Park, *J. Amer. Chem. Soc.* 127, 12498 **(2005)**.
17. K. Y. Lee, M. Katayama, S. Honda, T. Kuzuoka, T. Miyake, Y. Terao, J. G. Lee, H. Mori, T. Hirao, and K. Oura, *Jpn. J. App. Phys.* 42, L804 **(2003)**.
18. V. I. Merkulov, D. H. Lowdnes, Y. Y. Wei, G. Eres, and E. Voekl, *App. Phys. Lett.* 76, 3555 **(2000)**.
19. A. V. Melechko, V. I. Merkulov, T. E. McKnight, M. A. Guillorn, K. L. Klein, D. H. Lowdnes, and M. L. Simpson, *J. Appl. Phys.* 97, 041301 **(2005)**
20. B. O. Boskovic, V. Stolojan, R. U. A. Khan, S. Hag, and S. R. P. Silva, *Nature Mater.* 1, 165 **(2002)**.
21. A. C. Dillon, A. H. Mahan, P. A. Parilla, J. L. Alleman, M. J. Heben, K. M. Jones, and E. H. Gilbert, *Nano Lett.* 3, 1425 **(2003)**.
22. K. B. K. Teo, D. B. Hash, R. G. Lacerda, J. M. Meyyappan, and W. I. Milne, *Nano Lett.* 4, 921 **(2004)**.
23. M. H. Rummeli, E. Borowiak-Palen, T. Gemming, T. Pichler, M. Knupfer, M. Kalbac, L. Dunsch, O. Jost, S. R. P. Silva, W. Pompe, and B. Buchner, *Nano Lett.* 5, 1209 **(2005)**.
24. S. Hofmann, G. Csanyi, A. C. Ferrari, M. C. Payne, and J. Robertson, *Phys. Rev. Lett.* 95 **(2005)**.
25. J. V. Raty, F. Gygi, and G. Galli, *Phys. Rev. Lett.* 95, 096103 **(2005)**.
26. J. Gavillet, A. Loiseau, C. Journet, F. Willaime, F. Ducastelle, and J. C. Charlier, *Phys. Rev. Lett.* 87, 275504 **(2001)**.
27. H. J. Frost and M. F. Ashby, Deformation Mechanism Maps, Pergamon, Oxford **(1982)**.
28. W. W. Mullins, *J. Appl. Phys.* 28, 333 **(1957)**.
29. A. L. Giermann and C. V. Thompson, *App. Phys. Lett.* 86, 121903 **(2005)**.
30. M. Cantoro, S. Hofmann, S. Pisana, V. Scardaci, A. Parvez, C. Ducati, A. C. Ferrari, A. M. Blackburn, K. Y. Wang, and J. Robertson, *Nano Lett.* 6, 1107 **(2006)**.
31. P. L. Hansen, J. B. Wagner, S. Helveg, J. R. Rostrup-Nielsen, B. S. Clausen, and H. Topsoe, *Science* 295, 2053 **(2002)**.
32. S. Helveg, C. Lopez-Cartes, J. Sehested, P. L. Hansen, B. S. Clausen, J. R. Rostrup-Nielsen, F. Abild-Pedersen, and J. K. Norskov, *Nature* 427, 426 **(2004)**.
33. M. Lin, J. P. Y. Tan, C. Boothroyd, K. P. Loh, E. S. Tok, and Y. L. Foo, *Nano Lett.* 6, 449 **(2006)**.
34. T. D. Arcos, M. G. Garnier, J. W. Seo, P. Oelhafen, V. Thommen, and D. Mathys, *J. Phys. Chem. B* 108, 7728 **(2004)**.
35. S. Hofmann, R. Sharma, C. Ducati, G. Du, C. Mattevi, C. Cepek, M. Cantoro, S. Pisana, A. Parvez, F. Cervantes-Sodi, A. C. Ferrari, R. E. Dunin-Borkowski, S. Lizzit, L. Petaccia, A. Goldoni, and J. Robertson, *Nano Lett.* 7, 602 **(2007)**.
36. R. Sharma, P. Rex, M. Brown, G. Du, and M. M. J. Treacy, *Nanotechnology* 18, 1 **(2007)**.
37. S. Pisana, A. Jungen, C. Zhang, A. M. Blackburn, R. Sharma, F. Cervamtes, C. Stampfer, C. Ducati, A. C. Ferarri, C. Hierold, J. Robertson, and S. Hofmann, *J. Phys. Chem. C* **(2007)**.
38. H. W. Zhu, K. Suenaga, A. Hashimoto, K. Urita, K. Hata, and S. Iijima, *Small* 1, 1180 **(2005)**.
39. G. Eres, A. A. Kinhabwala, H. Cui, D. B. Geohegan, A. A. Puretzky, and D. H. Lowdnes, *J. Phys. Chem. B* 109, 16684 **(2005)**.
40. C. Klinke, J. M. Bonard, and K. Kern, *Phys. Rev. B* 71, 035403 **(2005)**.
41. A. Harutyunyan, T. Tokuna, and E. Mora, *App. Phys. Lett.* 87, 051919 **(2005)**.
42. F. Ding, K. Bolton, and A. Rosen, *J. Vac. Sci. Technol. A* 22, 1471 **(2004)**.
43. Y. Qi, T. Cagin, W. L. Johnson, and W. A. Goddard, *J. Chem. Phys.* 115, 385 **(2001)**.
44. K. Liu, K. L. Jiang, C. Feng, Z. Chen, and S. S. Fan, *Carbon* 43, 2850 **(2005)**.
45. M. Pinault, V. Pichot, H. Khodja, P. Launois, C. Reynaud, and M. M. L'Hermitage, *Nano Lett.* 5, 2394 **(2005)**.
46. X. Li, A. Cao, Y. J. Jung, R. Vajtai, and P. M. Ajayan, *Nano Lett.* 5, 1997 **(2005)**.
47. A. J. Hart and A. H. Slocum, *J. Phys. Chem. B* 110, 8250 **(2006)**.
48. S. Maruyama, R. Kojima, Y. Miyauchi, S. Chiashi, and M. Kohno, *Chem. Phys. Lett.* 360, 229 **(2002)**
49. Y. Murakami, S. Chiashi, Y. Miyauchi, M. Hu, M. Ogura, T. Okubo, and S. Maruyama, *Chem. Phys. Lett.* 385, 298 **(2004)**.
50. S. Maruyama, E. Einarsson, Y. Murakami, and T. Edamura, *Chem. Phys. Lett.* 403, 320 **(2005)**.
51. K. Hata, D. Futaba, K. Mizuno, T. Namai, M. Yumura, and S. Iijima, *Science* 306, 1362 **(2004)**.
52. D. N. Futaba, K. Hata, T. Yamada, K. Yamada, M. Yumura, and S. Iijima, *Phys. Rev. Lett.* 95, 056104 **(2005)**.
53. T. Yamada, T. Namai, J. Hata, D. N. Futaba, K. Mizuno, J. Fan, M. Yudasaka, M. Yumura, and S. Iijima, *Nat. Nanotechnol.* 1, 131 **(2006)**
54. D. N. Futaba, K. Hata, T. Namai, T. Yamada, K. Mizuno, Y. Hayamizu, and S. Iijima, *J. Phys. Chem. B* 110, 8035 **(2006)**.
55. S. Noda, K. Hasegawa, H. Sugime, K. Kakehi, Z. Zhang, S. Maruyama, and Y. Yamaguchi, *Jpn. J. Appl. Phys.* 46, L399 **(2007)**.
56. G. Zhong, T. Iwasaki, K. Honda, Y. Ohdomari, and H. Kawarada, *Jpn. J. App. Phys.* 44, 1558 **(2004)**.
57. T. Iwasaki, G. Zhong, and H. Kawarada, *J. Phys. Chem. B* 109, 19556 **(2005)**.
58. G. Zhong, T. Iwasaki, and H. Kawarada, *Carbon* 44, 2009 **(2006)**.
59. G. Zhong, T. Iwasaki, J. Robertson, and H. Kawarada, *J. Phys. Chem. B* 111, 1907 **(2007)**.
60. L. B. Zhu, Y. H. Xiu, D. W. Hess, and C. P. Wong, *J. Phys. Chem. B* 110, 5445 **(2006)**.
61. H. M. Christen, A. A. Puretzky, H. Cui, K. Belay, P. H. Fleming, D. B. Geohegan, and D. H. Lowdnes, *Nano Lett.* 4, 1939 **(2004)**.
62. G. Zhang, D. Mann, A. Javey, Y. Li, E. Yenilmez, Q. Wang, J. P. McVittie, Y. Nishi, J. Gibbons, and H. Dai, *Proc. Nat. Acad. Sci.* **(2005)**, Vol. 102, p. 16141.
63. Y. Q. Xu, E. Flor, H. Schmidt, R. E. Smalley, and R. H. Hauge, *App. Phys. Lett.* 89, 123116 **(2006)**.
64. L. Zhang, Y. Q. Tan, and D. E. Resasco, *Chem. Phys. Lett.* 422, 198 **(2006)**.

Received: 10 May 2007. Revised/Accepted: 3 October 2007.